Simulation and Modelling of Transient Electric Fields in HVDC Insulation Systems Based on Polarization Current Measurements

Pasquale Cambareri [1], **Carlo de Falco** [2], **Luca Di Rienzo** [1], **Paolo Seri** [3] and **Gian Carlo Montanari** [4,*]

1 Dipartimento di Elettronica, Informazione e Bioingegneria, Politecnico di Milano, 20133 Milano, Italy; pasquale.cambareri@polimi.it (P.C.); luca.dirienzo@polimi.it (L.D.R.)
2 MOX, Dipartimento di Matematica, Politecnico di Milano, 20133 Milano, Italy; carlo.defalco@polimi.it
3 Dipartimento di Ingegneria dell' Energia Elettrica e dell' Informazione, Università di Bologna, 40126 Bologna, Italy; paolo.seri2@unibo.it
4 Center for Advanced Power Systems, Florida State University, Tallahassee, FL 32306, USA
* Correspondence: gmontanari@fsu.edu

Abstract: Simulating and modelling electric field dynamics in the insulation of medium- and high-voltage DC electrical systems is needed to support insulation design optimization and to evaluate the impact of voltage transients on ageing mechanisms and insulation reliability. In order to perform accurate simulations, appropriate physical models must be adopted for the insulating material properties, particularly conductivity, which drives the electric field in a steady-state condition and contributes to determining the field behavior during voltage and load transients. In order to model insulation conductivity, polarization, and conduction, mechanisms must be inferred through charging and discharging current measurements, generally performed at different values of electric field and temperatures in flat specimens of the material under study. In general, both mechanisms are present, but one of them may be predominant with respect to the other depending on type of material. In this paper, we showed that models based on predominant polarization mechanisms were suitable to describe impregnated paper, but not polymers used for HV and MV DC insulation. In the latter case, indeed, trapping–detrapping and conduction phenomena were predominant compared to polarization, thus conductivity models had to be considered, in addition to or as a replacement of the polarization model, in order to carry out proper electric field simulations.

Keywords: HVDC insulation systems; DC cables; charging–discharging current modelling; electric fields

1. Introduction

The trend towards High Voltage Direct Current (HVDC) transmission, hybrid grids, renewable integration, and electrified transportation may cause weaknesses in grid and asset component reliability. This will hold, particularly for electrical insulation systems of existing components, such as cables, whose ageing is affected by voltage waveforms, DC and/or modulated AC, with repetitive or sporadic transients, harmonics, and ripples that might have not been accounted for the design stage. The consequence is an increase of the insulation ageing rate and loss of grid/asset component reliability (often incorrectly mentioned as "resilience") [1,2]. Therefore, there is a growing interest from insulation system designers and operators in diagnostic and maintenance, as well as in models and methods to evaluate ageing rate and health conditions of grid/asset components.

A basic need is the availability of accurate models for electric field calculation in insulation systems, which will help in gaining insights on the risk of triggering extrinsic ageing processes, such as partial discharges, especially during voltage transients [3]. Since conductivity drives the electric field under a DC steady state, and it contributes to determine the field behavior during transients (together with permittivity), measurement and modelling of conductivity behavior as a function of electric field and temperature constitutes the basis of building up accurate models. Specifically, the charging current contains mostly

information on the DC steady-state conduction mechanisms, while the discharging current provides information on the polarization and charge detrapping processes.

As an example of the importance of using accurate models for the simulation of electric fields, we refer to the results presented in [4], in which the effect of slow polarization processes on the electric field transient in HVDC paper-insulated cables was discussed. In [4], the standard model adopted for cable insulation, [5]; i.e.,:

$$
\begin{cases}
\nabla \cdot (\varepsilon_\infty \boldsymbol{E}) = \rho \\
\frac{\partial \rho}{\partial t} + \nabla \cdot (\sigma \boldsymbol{E}) = 0
\end{cases} ,
\tag{1}
$$

where $\boldsymbol{E}$ is the electric field, ρ is the charge density, ε_∞ is the permittivity of fast polarization processes (such as dipolar polarization), and σ is the temperature- and field-dependent conductivity, and is extended using the Debye relaxation equation:

$$
\tau_k \frac{\partial \boldsymbol{P}_k}{\partial t} + \boldsymbol{P}_k = \varepsilon_0 \chi \boldsymbol{E} ,
\tag{2}
$$

where $\boldsymbol{P}_k$ is the polarization vector of the k-th polarization process, while τ_k is the time constant and χ_k is the susceptivity. As shown in [4], the polarization dynamic slows down the electric field transient, yielding non-negligible differences between the predictions of the standard model (1) and the one extended with the Debye Equation (2).

Figure 1, for example, shows the maximum electric field in a HVDC paper-insulated cable during energization, polarity inversion, and discharge. The transient maximum field predicted by the polarization model is lower than the one provided by the standard model during energization and polarity inversion transients. At steady state, the two fields reach the same value. It can be speculated that the lower transient field may imply a lower risk of triggering extrinsic ageing phenomena during transients, or lower time and magnitude for PD occurrence, hence the expected life of the cable estimated from the two models may be different.
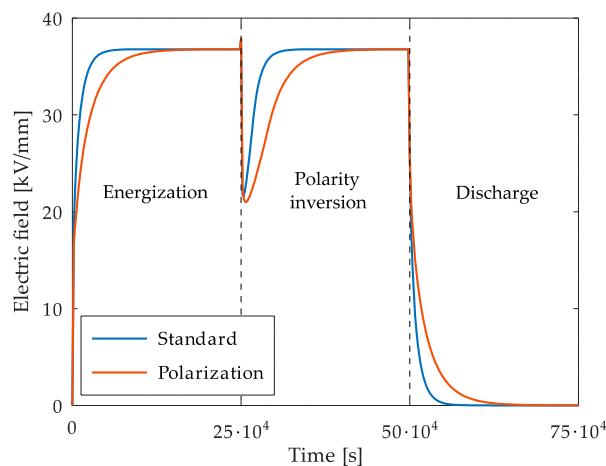
Figure 1. Simulation of the maximum insulation electric field in a HVDC paper-insulated cable, with rated voltage 300 kV, insulation thickness 20 mm, and conductor radius 23 mm, during energization, polarity inversion, and discharge, using both the standard model (1) and one that includes slow polarization processes (2). Maximum temperature 55 °C, temperature gradient 30 °C. Relative permittivity $\varepsilon_\infty = 3.5\varepsilon_0$, conductivity $\sigma(T) = \sigma_0 \cdot \exp\left[-\alpha\left(T^{-1} - T_{ref}^{-1}\right)\right]$, with $\sigma_0 = 3.21 \cdot 10^{-14}$ S, $\alpha = 1.01 \cdot 10^4$ K, and $T_{ref} = 50$ °C. Time constants: $\tau_1 = 13.2$, $\tau_2 = 35.7$, $\tau_3 = 3120$; susceptibilities $\chi_1 = 0.401$, $\chi_2 = 1.970$, and $\chi_3 = 2.460$. See Equation (2).

Under DC excitation, dipolar and interfacial polarization takes part in the charging process of both impregnated paper and polymers (solid dielectrics). In impregnated paper, interface charge accumulated between the paper layers and the impregnant can predominate at lower frequency, while dipolar relaxation mechanisms play a role at higher

frequencies. In polymers, the charge carrier can gather at the interfaces between crystalline, semicrystalline, and amorphous regions, as well as in chemical traps, being resident for much longer times than oil–paper insulation (due to deeper trap depth). From a mathematical point of view, interfacial and dipolar polarization is usually described by the extended Debye model, which postulates the existence of a number of parallel processes, each of which is accounted for by an equation of the form (2). This model is generally employed to fit the polarization and depolarization currents measured under DC excitation in both impregnated paper [6–8] and polymers [9–13]. However, while in impregnated paper there is good confidence that interfacial polarization is the dominant relaxation process, and hence the extended Debye model can be regarded as a suitable physical description of the material rather than just a mathematical tool, in the case of polymers, its validity may be questionable due to the presence of other mechanisms, such as charge trapping and detrapping. These latter mechanisms may prevail on polarization, and hence they require a different physical and mathematical description.

Modern methodologies for the simulation of electric fields in solid dielectrics do not consider polarization processes, but focus on bipolar charge transport (BCT) models (see, for example, [14–17]). These models describe the motion of two charge carriers (electrons and holes) through the bulk of the dielectric by means of the drift–diffusion equations. The transport dynamic of such carriers is influenced by charge recombination and trapping and detrapping processes, which are considered by means of the continuity equation. It is generally assumed that the mobile carriers are injected from the electrodes, while internal generation is often neglected. The main limitation of these models, however, is that they require a considerable number of parameters that are quite difficult to estimate from experimental measurements of charging and discharging currents.

The purpose of this paper was to show that, while the extended Debye model can be a suitable physical and mathematical description for polarization and depolarization currents measured in impregnated paper under DC excitation, it is not as effective, in general, for polymers, for which a new modelling approach is needed.

2. Model-Fitting Procedure and Validation Criteria

The circuital version of the extended Debye model is depicted in Figure 2. In this article, we will also refer to it as the Occhini equivalent circuit, after [6]. This circuital model is valid under the assumption that no space charge is accumulated in the dielectric. In case of polymers, this is true if the electric field remains below the space charge accumulation threshold [18]. In this article, we use it to describe the polarization and depolarization currents measured from the DC excitation of thin flat samples of dielectric materials with thickness d and area A.
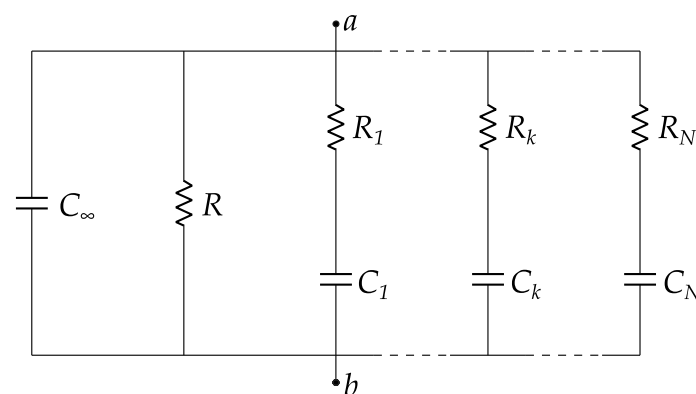
Figure 2. The Occhini equivalent circuit (or extended Debye model).

In Figure 2, resistance R accounts for the DC steady-state conduction mechanism. Parallel branches R_k-C_k model the dipolar and interfacial polarization, characterized by the time constant $\tau_k = R_k C_k$. The faster mechanisms, however, cannot be inferred by DC
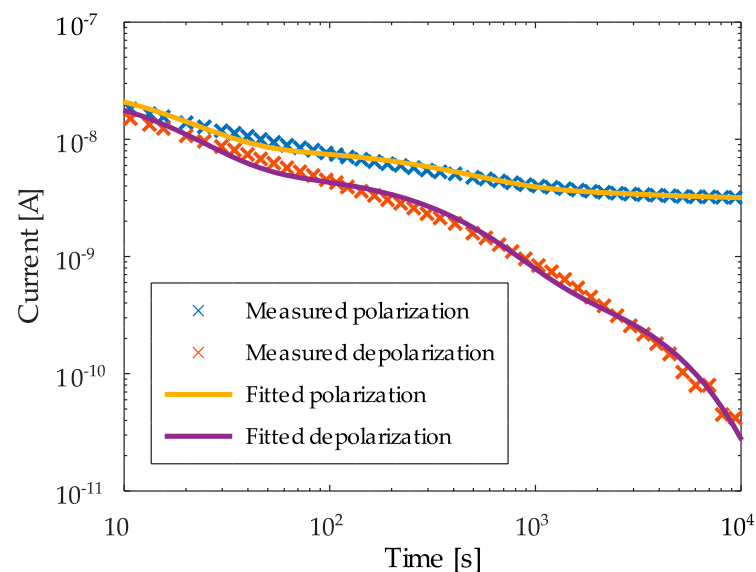
current measurements, because the DC generator operation overlaps on the specimen dielectric response, thus they are accounted for via the capacitance C_∞, which can be estimated by means of dielectric spectroscopy measurements at relatively high frequency; e.g., 1 Hz or above [19]. Resistance R is calculated dividing the steady-state polarization current by the voltage applied to the dielectric sample. Branches R_k-C_k can be fitted either from the polarization transient current, or from the depolarization one (see Figure 3 as an example).

Regardless of the adopted procedure, we can devise a simple criterion to the determine whether the Occhini circuit is suitable for modeling the sample under test. If branches R_k-C_k are fitted from the depolarization current, the simulation of the polarization current must be compatible with the measured one. Vice versa, if the branches are fitted from the polarization current, the simulation of the depolarization one must be compatible with the experiment. The techniques used in this article to determine the values of resistances R_k and capacitances C_k are described in [4,20,21]. The link between the differential model parameters in (1) and (2) and the circuital parameters in Figure 2 is provided by the following relationships:

$$\varepsilon_\infty = C_\infty \cdot \frac{d}{A} \, , \tag{3}$$

$$\sigma = \frac{1}{R} \cdot \frac{d}{A} \, , \tag{4}$$

$$\chi_k = \frac{C_k}{\varepsilon_0} \cdot \frac{d}{A} \, . \tag{5}$$

Figure 3. Fitting polarization and depolarization current in impregnated paper using the Occhini equivalent circuit. Experimental data were from [22].

If the circuital parameters are fitted from the polarization and depolarization curves; i.e., the model is valid, then the parameters of the differential model are retrieved through (3)–(5) and the electric field transient in the cable is simulated by Equations (1) and (2).

3. Impregnated Paper

Figure 3 shows an example of the capability of the Occhini equivalent circuit to describe charging and discharging current curves in oil-impregnated paper. The experimental depolarization current, taken from [18] and relevant to paper–oil specimens, is described accurately through the circuit of Figure 2, using three R_k-C_k branches (data reported in [22] came from conductivity measurements performed at 30.6 kV on a mass-impregnated specimen 2.45 mm thick and with an area of 78.54 cm^2).

Branches R_k-C_k were fitted to the measured depolarization current in Figure 3, using the procedure described in [4]. The fact that only three branches were sufficient to obtain a qualitatively acceptable fitting may have been an indication that the most significant polarization processes could be identified using the Occhini model representation of Figure 2. Table 1 reports the capacitance, resistance, and time constant values. Model validity was confirmed by the fact that the circuit parameters thus determined could provide very good fitting also for charging (polarization) currents, provided that the contribution of the DC current, accounted for by the resistance R, was added. The fitted value for this resistance was $9.71 \cdot 10^{12}$ Ω. It can be speculated, therefore, that the model of Figure 1, derived from Occhini's approach, could successfully describe mass-impregnated and fluid-oil impregnated paper.

Table 1. Fitting of experimental polarization and depolarization currents in impregnated paper using three R_k -C_k branches in the Occhini circuit.

| k	R_k (Ω)	C_k (F)	τ_k (s)
1	1.16×10^{12}	1.14×10^{-11}	1.32×10^{1}
2	6.39×10^{12}	5.58×10^{-11}	3.57×10^{2}
3	4.47×10^{13}	6.98×10^{-11}	3.12×10^{3}

4. Polymeric Solid Insulation

As described in the previous section, the Occhini circuit could be successfully applied to describe the behavior of impregnated paper insulation, in which polarization mechanisms constituted the predominant processes for charging and discharging current transients. Here, we showed that this model might not be adequate to describe solid polymeric dielectric materials, such as polypropylene (PP) or polyethylene (PE), based on experimental results of polarization and depolarization current measurements. Further studies are then required to investigate transient charge trapping/detrapping mechanisms in solid polymers used for DC insulation to achieve a proper description of the electric field distribution during voltage transients.

Charging and discharging currents were measured under electric field values up to 30 kV/mm and at a temperature of 60 °C with a custom setup comprising a high-voltage DC source (FUG HCN 35–35000), an electrometer (Keysight B2980A, Keysight Technologies, Santa Rosa, CA, USA), and a conductivity measurement cell built in-house. The adopted system had a resolution of 0.001 pA, with a background noise of 0.1 pA. Specimens were made of polypropylene (PP) that was thermally pretreated, and had gold sputtered electrodes with a diameter of 26 mm and a guard ring (Figures 4 and 5).
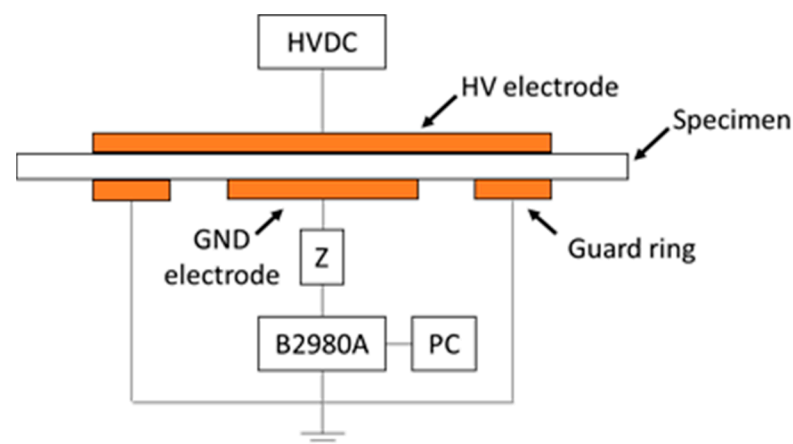
Figure 4. Scheme of the experimental setup used to measure charging and discharging currents in solid polymers.
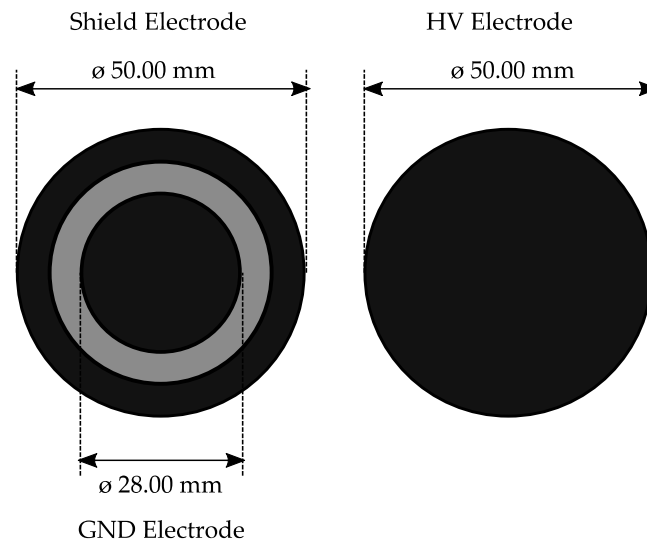
Figure 5. Geometric sizes of the high-voltage electrode, the ground electrode, and the shield electrode (guard ring).

If the same fitting procedure adopted for impregnated paper was applied to charging and discharging current measurements collected by the above experimental setup for solid polymers, we could observe an unsatisfactory description of the conduction current, as shown in Figure 6. This figure was obtained from tests at 15 kV and 60 °C on a sample 0.5 mm thick. The parameter values of the three R_k-C_k branches composing the Occhini model are reported in Table 2. Capacitance C_∞ was $4 \cdot 10^{-11}$ F, while resistance R was $6 \cdot 10^{13}$ Ω as obtained from the DC steady-state measured current. The generator of the experimental setup had a transient behavior that is well described by an exponential:

$$v_g(t) = V \cdot e^{-\frac{t}{\tau_g}} , \qquad (6)$$

where V is the magnitude of the applied voltage and τ_g is the generator time constant, equal to 2.5 s.
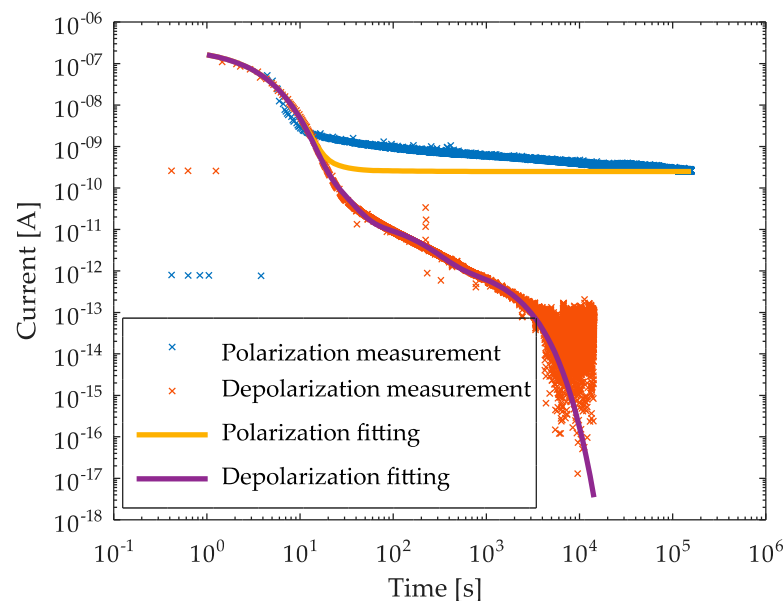
Figure 6. Fitting of the depolarization (discharging) current using the Occhini circuit for three branches. The resulting parameters, however, did not fit the polarization current.

Table 2. Fitting of the experimental depolarization current in PP using three R_k-C_k branches in the Occhini circuit.

| k	R_k (Ω)	C_k (F)	τ_k (s)
1	1.56×10^{13}	6.61×10^{-13}	1.03×10^1
2	8.58×10^{14}	1.40×10^{-13}	1.20×10^2
3	9.96×10^{15}	1.10×10^{-13}	1.10×10^3

As observed from Figure 6, the simulated polarization current reached its steady-state value much faster than the experimental curve. The explanation for this observed behavior can be understood by considering that the ratio between the depolarization current of the k-th branch in the Occhini model, $i_k(t)$, and the conduction current, i_{cond}, is:

$$\frac{i_k(t)}{i_{cond}} = \frac{C_k \cdot V / \tau_k \cdot e^{-t/\tau_k}}{V/R} = \frac{R}{R_k} \cdot e^{-\frac{t}{\tau_k}} . \tag{7}$$

where the resistances R_k fitted from the experimental depolarization current, see Table 2, have values close to or even larger than R:

$$\frac{R_1}{R} \simeq 0.26, \quad \frac{R_2}{R} \simeq 14, \quad \frac{R_3}{R} \simeq 166, \tag{8}$$

especially for the longer time constants. Therefore, as can be inferred from (7), in the simulated polarization transient, the conduction current was so large that it overwhelmed the polarization ones. This was a first indication that the Occhini model might not be suitable to describe conduction and field distribution of solid dielectric polymers used for DC application, especially in cables. The same unsatisfactory result, as shown in Figure 7, was obtained if the opposite procedure was applied; i.e., fitting the polarization transient current and, with obtained parameter values, retrieving the depolarization current. The values of C_{inf} and R were the same as in the simulation shown in Figure 6, while the parameters R_k-C_k were fitted again (see Table 3).
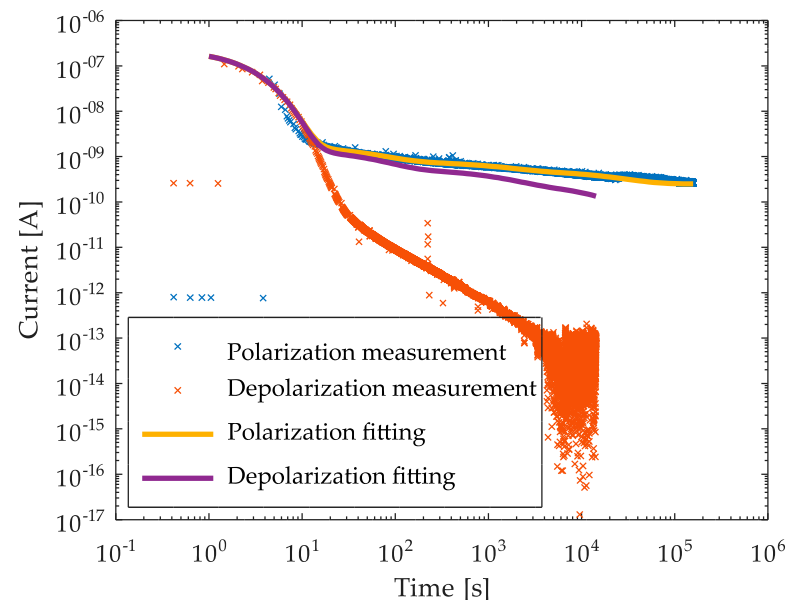
Figure 7. Fitting of the polarization current in PP though Occhini model for three branches. The model using the parameters thus estimated did not fit the depolarization current.

Table 3. Fitting of the experimental polarization current in PP using three R_k-C_k branches in the Occhini circuit.

| k	R_k (Ω)	C_k (F)	τ_k (s)
1	1.62×10^{13}	3.65×10^{-12}	5.91×10^1
2	5.26×10^{14}	2.61×10^{-11}	1.37×10^2
3	6.18×10^{15}	3.90×10^{-10}	2.41×10^3

To confirm that the Occhini equivalent circuit may not be able to model dielectric polymers, we attempted to increase the number of R_k-C_k branches. To this aim, the much more complex fitting procedure described in [20,21] could be applied. This approach is based on approximating the depolarization current as:

$$i_{dep}(t) = \sum_{k=1}^{N} A_k \, e^{-t/\tau_k} \, , \tag{9}$$

which corresponds to the total current at node b when the nodes in Figure 2 were short-circuited; i.e., the sum of all the currents in the R_k-C_k branches. The procedure worked as follows:

1. large number N of time constants τ_k uniformly distributed in logarithmic scale was considered;
2. Coefficients A_k that exactly matched the measured values of the depolarization current in the corresponding time instants were computed;
3. Time constants corresponding to negative values of A_k were removed;
4. The process was iterated until all the obtained A_k were positive.

In our case, $N = 500$ time constants τ_k were chosen between 3 s and $4 \cdot 10^4$ s, and the interpolation procedure ended with $N = 7$ relaxation times. Capacitance C_∞ and resistance R were the same as in the previous attempts: branches R_k-C_k indeed were used to fit only the slow polarization processes. Figure 8 shows that while the fitting of the discharging process was good, it was still not sufficient to reconstruct the polarization current. Figures 9 and 10 report, respectively, the fitted resistances R_k and capacitances C_k versus the τ_k.
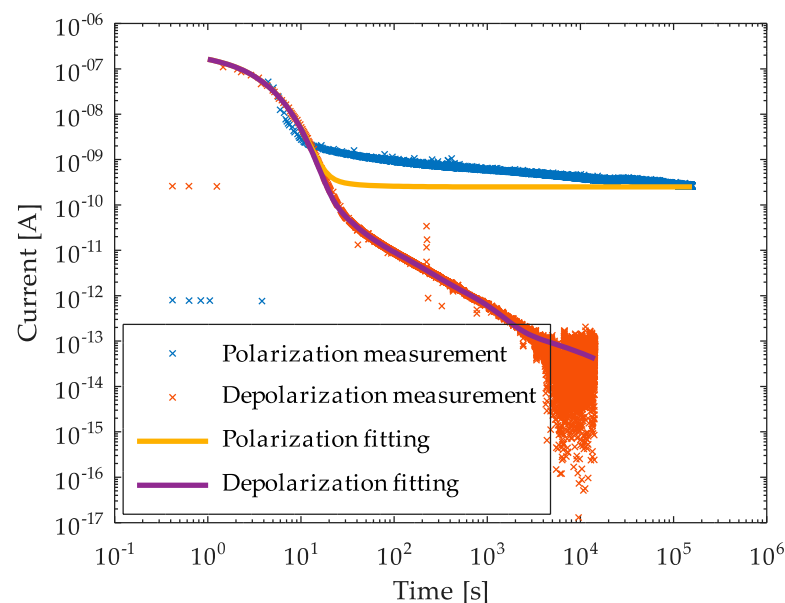
Figure 8. Fitting of the depolarization current through Occhini's model with an increased number of branches (see Equation (9)). The model using the parameters thus estimated did not fit the polarization current.
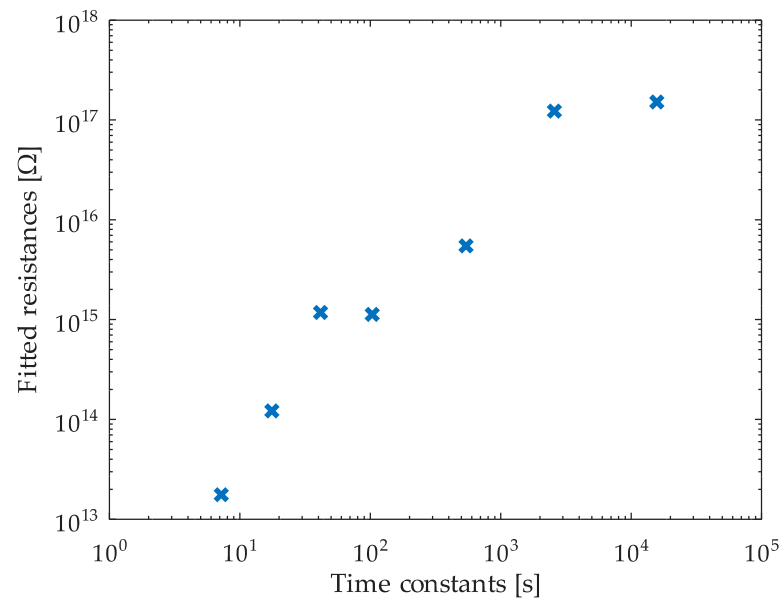
Figure 9. Fitted resistances R_k in PP using the approach in [20,21] versus time constants τ_k.
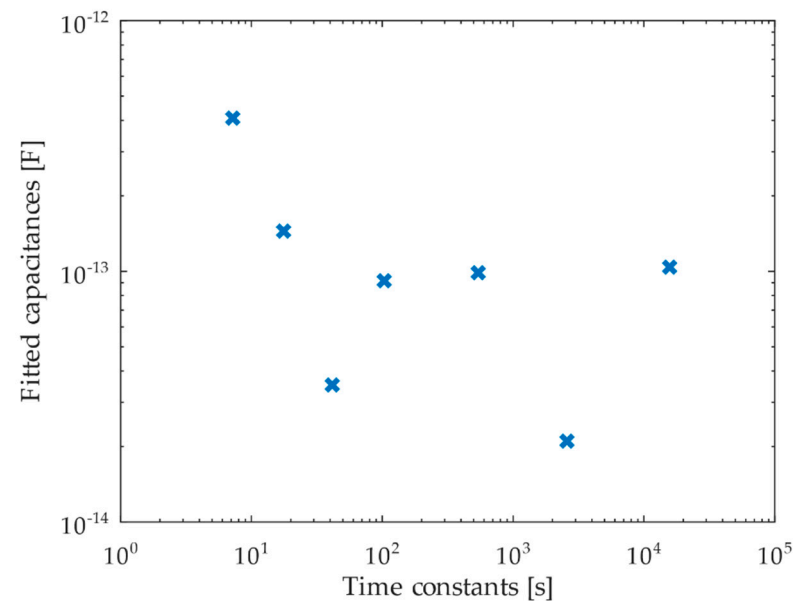

Figure 10. Fitted capacitances C_k in PP using the approach in [20,21] versus time constants τ_k.

5. Discussion

The results presented in Section 3 indicated that the Occhini equivalent circuit was a suitable model to describe polarization and depolarization currents in impregnated paper insulation. The validity of the model supported the idea that the charging process in this type of insulation was governed by the surface charge that was stored at the interface between the paper layers and the impregnant. This was, indeed, the interpretation given by Occhini and Maschio in [6]. Hence, the use of the Occhini circuit, which introduced the time-dependent permittivity, could positively impact the description of the insulation electric field profile of an HVDC cable during voltage transients with respect to a model featuring constant permittivity (and conductivity) [4]. On the other hand, it was shown in Section 4 that the same may not be suitable to achieve an accurate description of the field transient of polymeric solid insulating materials. With reference to Table 2, the polarization resistance R_1, associated with the shortest time constant, was one order of magnitude smaller than resistance R, which related to the DC conduction mechanism. This indicated

that in the initial portion of charging and discharging transients, polarization mechanisms may have been significant, and this could be accounted for by one R_k-C_k branch of the Occhini model. For longer times, however, resistances R_2 and R_3 exceeded the value of R by at least two orders of magnitude: in this case, the polarization currents predicted by the Occhini model was not able to fit the experimental current behavior with physically meaningful values. For long times, branches associated to R_2 and R_3 must then be replaced with a different model that takes into account the contribution of a transient current that is to be ascribed to trapping and detrapping mechanisms.

6. Conclusions

The main contribution of this paper was to highlight how effective models are still lacking that properly describe the experimental behavior of insulating materials for DC applications. In particular, the time behavior of the electric field profile and magnitude can change noticeably when referring to the dynamic model illustrated here, in comparison to the static approach (1) generally used [4,23–25]. Knowing the real value of the electric field during the transient following, e.g., a voltage polarity inversion, is functional to carry out reliable insulation system design that is partially discharge free, and address the specified life and failure probability [2,3]. However, while the dynamic model illustrated here, based on the Debye model, worked well for oil-impregnated paper, it may not properly describe polymeric materials. Thus, more complex models, stemming from the fit of charging–discharging currents measured at different field and temperatures, must be considered and developed. The inherent complication is that models must fit to the conduction and polarization processes, since insulating materials exhibit both time-dependent electric permittivity, due to the polarization process, and time-dependent electric conductivity, which is associated with trapping/detrapping conduction mechanisms.

In conclusion, the modelling of materials in which polarization mechanisms are predominant, particularly impregnated paper, found solid foundation in the Occhini equivalent circuit as introduced and inferred here. As for polymeric materials, which in fact represent the state of the art for DC insulation system technology, additional work is required to complete the model with a suitable description of transient phenomena associated with trapping and detrapping conduction mechanisms.

Author Contributions: Conceptualization, G.C.M.; investigation, P.C., P.S., C.d.F., L.D.R. and G.C.M.; methodology, P.C., P.S. and C.d.F.; supervision, P.S., C.d.F., L.D.R. and G.C.M.; writing—original draft, P.C., C.d.F., L.D.R., P.S. and G.C.M.; writing—review and editing, P.C., C.d.F., L.D.R., P.S. and G.C.M. All authors have read and agreed to the published version of the manuscript.

Institutional Review Board Statement: Not applicable.

Informed Consent Statement: Not applicable.

Data Availability Statement: Not applicable.

Abbreviation

Notation table with the symbols used in this paper:

Symbol	Description
ε_∞	Dielectric permittivity, referred to high-frequency processes (1 Hz or above)
E	Electric field in the dielectric
ρ	Charge density in the dielectric
σ	Electric conductivity
P_k	Polarization vector of the k-th polarization process in the Debye model

τ_k	Time constant of the *k*-th polarization process in the Debye model
χ_k	Dielectric susceptivity of the *k*-th polarization process in the Debye model
ε_0	Dielectric permittivity of vacuum
C_∞	Capacitance of the Occhini circuit associated with permittivity ε_∞
R	Steady-state resistance of the Occhini circuit associated with conductivity σ
R_k	Resistance of the Occhini circuit associated with the *k*-th polarization process
C_k	Capacitance of the Occhini circuit associated with the *k*-th polarization process

References

1. Montanari, G.C.; Morshuis, P.; Seri, P.; Ghosh, R. Ageing and reliability of electrical insulation: The risk of hybrid AC/DC grids. *High Volt.* **2020**, *5*, 620–627. [CrossRef]
2. Montanari, G.C.; Ghosh, R.; Naderiallaf, H.; Seri, P. Reliability of HVDC and MVDC electrical asset: The challenge of insulation design. In Proceedings of the 2021 IEEE International Conference on the Properties and Applications of Dielectric Materials (ICPADM), Johor Bahru, Malaysia, 12–14 July 2021.
3. Naderiallaf, H.; Seri, P.; Montanari, G.C. Designing a HVDC insulation system to endure electrical and thermal stresses under operation. Part I: Partial discharge magnitude and repetition rate during transients and in DC steady state. *IEEE Access* **2021**, *9*, 35730—35739.
4. Cambareri, P.; de Falco, C.; Di Rienzo, L.; Seri, P.; Montanari, G.C. Charging and discharging current measurements and impact of polarization dynamics on electric field modeling in HVDC paper-insulated cables. *IEEE Access* **2021**, *9*, 45155–45162. [CrossRef]
5. Jeroense, M.J.P.; Morshuis, P.H.F. Electric fields in HVDC paper-insulated cables. *IEEE Trans. Dielectr. Electr. Insul.* **1998**, *5*, 225–236. [CrossRef]
6. Occhini, E.; Maschio, G. Electrical characteristics of oil-impregnated paper as insulation for HV DC cables. *IEEE Trans. Power App. Syst.* **1967**, *86*, 312–326. [CrossRef]
7. Saha, T.K.; Purkait, P.; Muller, F. Deriving an equivalent circuit of transformers insulation for understanding the dielectric response measurements. *IEEE Trans. Power Deliv.* **2005**, *20*, 149–157. [CrossRef]
8. Yang, F.; Du, L.; Yang, L.; Wei, C.; Wang, Y.; Ran, L.; He, P. A parameterization approach for the dielectric response model of oil paper insulation using FDS measurements. *Energies* **2018**, *11*, 622. [CrossRef]
9. Cheng, X.; Ye, G.; Sun, H.; Li, T.; Sun, C. Analysis of low-frequency dielectric loss of XLPE cable insulation based on extended Debye model. *AIP Adv.* **2021**, *11*, 085103. [CrossRef]
10. Morsalin, S.; Phung, B.T. Dielectric response study of service-aged XLPE cable based on polarisation and depolarisation current method. *IEEE Trans. Dielectr. Electr. Insul.* **2020**, *27*, 58–66. [CrossRef]
11. Zhang, Y.-Y.; Jiang, F.-Y.; Yu, X.-Y.; Zhou, K.; Zhang, W.; Fu, Q.; Hao, J. Assessment of thermal aging degree of 10kV cross-linked polyethylene cable based on depolarization current. *IEEE Access* **2021**, *9*, 111020–111029. [CrossRef]
12. Morsalin, S.; Phung, B.T. Dielectric response measurement on service-aged XLPE cables: From very low frequency to power frequency. *IEEE Electr. Insul. Mag.* **2020**, *36*, 19–31. [CrossRef]
13. Lin, S.; Zhou, K.; Li, M. *A Space Charge Measurement Method of XLPE Based on Polarization and Depolarization Current*; IEEE Electrical Insulation Conference (EIC): Knoxville, TN, USA, 2020.
14. Doedens, E.; Jarvid, E.M.; Guffond, R.; Serdyuk, Y.V. Space Charge Accumulation at Material Interfaces in HVDC Cable Insulation Part I—Experimental Study and Charge Injection Hypothesis. *Energies* **2020**, *13*, 2005. [CrossRef]
15. Doedens, E.; Jarvid, E.M.; Guffond, R.; Serdyuk, Y.V. Space Charge Accumulation at Material Interfaces in HVDC Cable Insulation Part II—Simulations of Charge Transport. *Energies* **2020**, *13*, 1750. [CrossRef]
16. Jörgens, C.; Clemens, M. A Review about the Modeling and Simulation of Electro-Quasistatic Fields in HVDC Cable Systems. *Energies* **2020**, *13*, 5189. [CrossRef]
17. Ren, H.; Gao, H.; Li, C.; Li, Q.; Wang, Z. Numerical research on space charge inside solid dielectrics under unipolar and bipolar voltage conditions. *IEEE Trans. Dielectr. Electr. Insul.* **2021**, *28*, 98. [CrossRef]
18. Montanari, G.C. The electrical degradation threshold of polyethylene investigated by space charge and conduction current measurements. *IEEE Trans. Dielectr. Electr. Insul.* **2000**, *7*, 309. [CrossRef]
19. Jonscher, A.K. *Dielectric Relaxation in Solids*; Chelsea Dielectric Press Ltd.: London, UK, 1983; pp. 47–52.
20. Der Houhanessian, V.; Zaengl, W.S. Time domain measurements of dielectric response in oil-paper insulation systems. In Proceedings of the Conference Record of the 1996 IEEE International Symposium on Electrical Insulation, Montreal, QC, Canada, 16–19 June 1996.
21. Der Houhanessian, V. Measurement and Analysis of Dielectric Response in Oil-Paper Insulation Systems. Ph.D. Thesis, ETH Zurich, Zurich, Switzerland, 1998.
22. Hakonseth, G.; Ilstad, E. Time–dependent electric field distribution in layered paper-oil insulation. In Proceedings of the 26th Nordic Insulation Symposium, Tampere, Finland, 5 August 2019.
23. Cambareri, P.; de Falco, C.; Di Rienzo, L.; Seri, P.; Montanari, G.C. Electric field calculation during voltage transients in DC cables: The contribution of polarization processes. *IEEE Trans. Dielectr. Electrc. Insul.* **2022**. under review.

24. Cambareri, P.; de Falco, C.; Di Rienzo, L.; Seri, P.; Montanari, G.C. Finite difference and equivalent circuit modelling of polarization in HVDC cables. In Proceedings of the 23rd International Conference on the Computation of Electromagnetic Fields COMPUMAG 2021, Cancun, Mexico, 16–20 January 2022.
25. de Falco, C.; Cambareri, P.; Di Rienzo, L.; Seri, P.; Montanari, G.C. Field transients in HVDC insulation materials: Hierarchical finite element modelling. In Proceedings of the 23rd International Conference on the Computation of Electromagnetic Fields COMPUMAG 2021, Cancun, Mexico, 16–20 January 2022.